National Radio Astronomy Observatory
EVLA Memo #234

Design and Measurement of New Cross-guide Directional Couplers for the Ka-band Receiver

B. DuVerneay, J. Allison, W. Grammer (NRAO)

August 13, 2024

Contents

Introduction

The Expanded Very Large Array Project (EVLA) upgrade to the Karl G. Jansky Very Large Array (VLA) utilized a "cross-guide" waveguide directional coupler to inject a noise signal for gain calibration before the Low Noise Amplifier (LNA) in the K-band and Ka-band receivers. This device is often referred to as a "Calibration Coupler" or "Cal Coupler" as part of the EVLA project. A block diagram for the EVLA Ka-band receiver is shown with the directional couplers identified in the signal path in Figure 1.

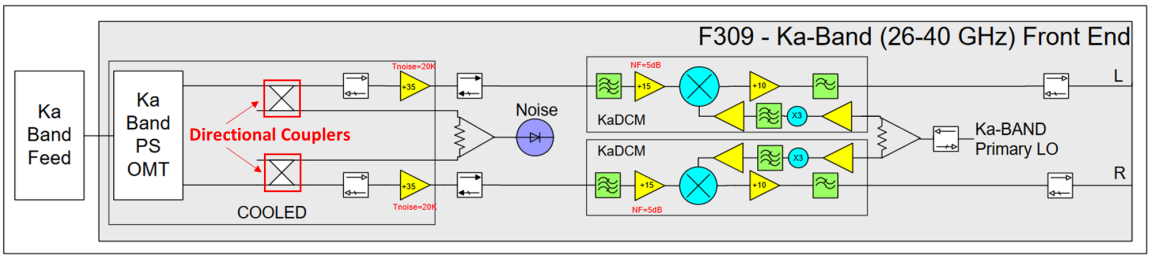

Figure 1. EVLA Ka-band receiver front-end block diagram [1]

The original Cal Coupler consisted of 3 major parts that were soldered together, surfaced, and gold-plated. Excellent performance can be achieved in these soldered devices when the manufacturing steps are carried out perfectly, however, the process is very time-consuming and cumbersome. Voids in the solder lead to gaps in the waveguide H-plane (where broad-wall meets narrow-wall), which create unacceptable resonances in the Thru (S21) transmission response in-band. This apparently occurred frequently during production and yields of just 75% or less were achieved. (B. Willoughby, personal communication, 27 October 2022).

This effort seeks to re-design these directional couplers so that they are assembled using fasteners, rather than solder. These devices can be spares for EVLA replacements in the K-band and Ka-band receiver designs. This effort can also inform directional coupler designs for use in the next generation Very Large Array (ngVLA). The goals are to design for manufacturing, including:

- Achieve high component yield and low scrap.
- Simplify the cumbersome fabrication and assembly process.
- Lower cost by reducing time to fabricate each unit and improving yield.
- Review existing drawing tolerances and refine where appropriate.

Note that an improvement in performance compared to a well-performing soldered device is not the expected goal, as a perfectly assembled unit with parts very close to the nominal drawing dimensions performs quite well in the existing EVLA receivers.

Cross-guide Directional Coupler Design Basics

Cross-guide couplers are also known as "Moreno" couplers, since A. Moreno is credited with the original design idea in 1946 [2]. These devices utilize two waveguides placed perpendicular to one another with two small "holes" or "apertures" in the broad-wall of the waveguides which allows for electromagnetic fields to couple from one waveguide to the other. Various shapes of apertures have been studied, but "cross-shaped" (looks like an "X" or "+") is most frequent and able to achieve flat coupling and directivity over the waveguide bandwidth [3]. A top view of the

structure is shown in Figure 2. The coupling apertures are located so that the path length from plane A to plane B for the wave coupled through one aperture is equal to the path length for the wave coupled through the second aperture. This results in cancellation in the B direction, since the coupled fields through each aperture are designed to be 180 degrees out of phase. This is not the case in the C direction, and cancelation will not occur [4] . The size and location of the apertures largely determines the s-parameters of the device.

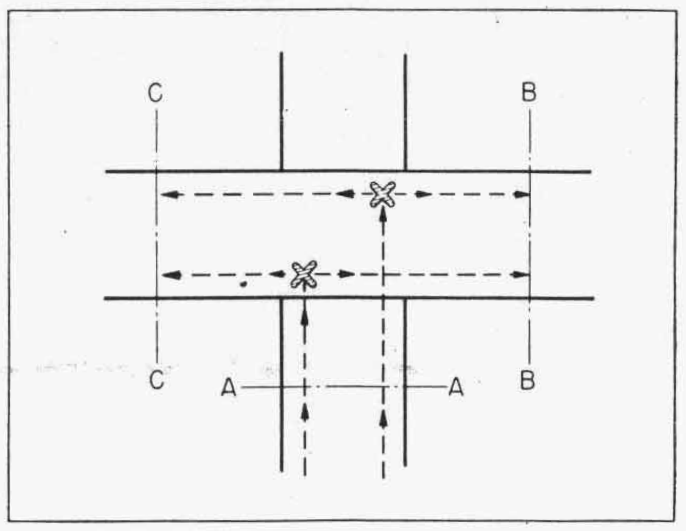

Figure 2. Cross-guide coupler, plan view [4]

Some of the advantages of cross-guide couplers are size, cost, low insertion loss, and fairly good directivity. Other larger coupler designs which employ parallel waveguides with many apertures can achieve higher directivity or flatter coupling over a broader bandwidth, but at the expense of the advantages of the cross-guide coupler design. Cross-guide couplers excel with low coupling factors, as is commonly used in gain calibration for radio astronomy receivers in order to minimize receiver noise temperature. Extremely flat coupling over a wide bandwidth is typically not required for calibration. While the injected noise in EVLA is equivalent to approximately 5% of the nominal system temperature T_{sys} [1], a limit on variation over frequency is not clearly defined; a factor of 2 variation in the noise power to system temperature ratio over frequency is generally considered reasonable, with only a small degradation in system sensitivity as a consequence. In general, the cross-guide coupler is a good fit for radio astronomy gain calibration applications, especially when available space is limited.

Key performance parameters for this 4-port device over the frequency band are:

- Insertion Loss (S21): Minimize receiver noise temperature.
- Return Loss (S11, S22, S33, S44): Minimize mismatch loss and gain ripple.
- Coupling Factor Flatness (S31): “Relatively” flat. Flatness has an impact on system sensitivity during a calibration cycle (variation in noise power over frequency leads to degradation in T_{sys}).
- Directivity (S31-S41): “Good” directivity to minimize energy radiated out of the antenna and standing waves in the receiver front-end.
- High Reliability operation at cryogenic temperatures, ability to survive many temperature cycles without maintenance.

Original EVLA Design

An isometric view of a final assembled Ka-band EVLA coupler, part number 23140A0006 Rev B is shown in Figure 3

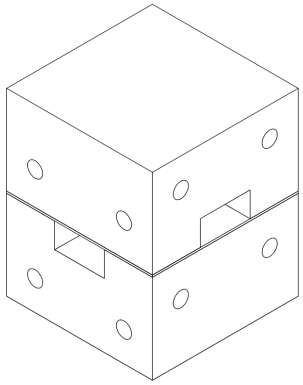

Figure 3. EVLA cross-guide "Cal Coupler" assembly

This assembly is composed of the two waveguide half blocks and a thin plate between them which contains the coupling apertures. This thin coupling aperture plate from the Ka-band (23140M0010 Rev E) and K-band (23145M0041-2 Rev B) drawings are shown in Figure 4 and Figure 5, respectively. Note that all dimensions are in inches and are to three decimal places, except for the alignment pin locations. The tolerance for three-decimal place dimensions are ±0.005 inches.

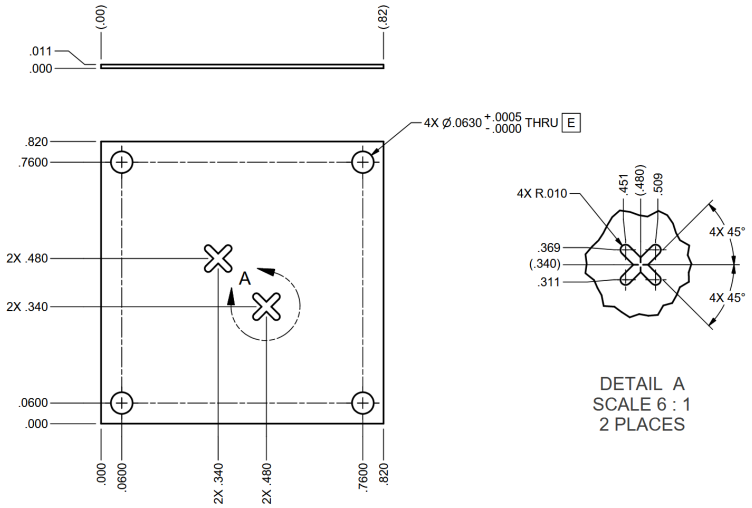

Figure 4. Ka-band Coupling Aperture Plate drawing

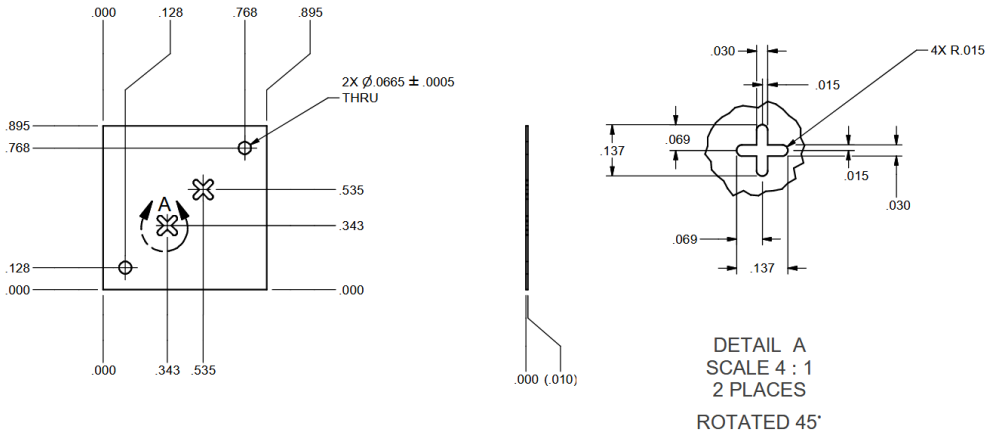

Figure 5. K-band Coupling Aperture Plate drawing

The mechanical assembly for each of the Ka-band and K-band designs is essentially the same. The assembly drawing 23145A0015 for the "K-band Cal Coupler Assembly" shows the process of assembling the unit, which involves a well-documented, but somewhat cumbersome soldering process (Process 2) and machine shop re-surfacing and gold plating (Process 3). An excerpt from the drawing is shown in Figure 6.

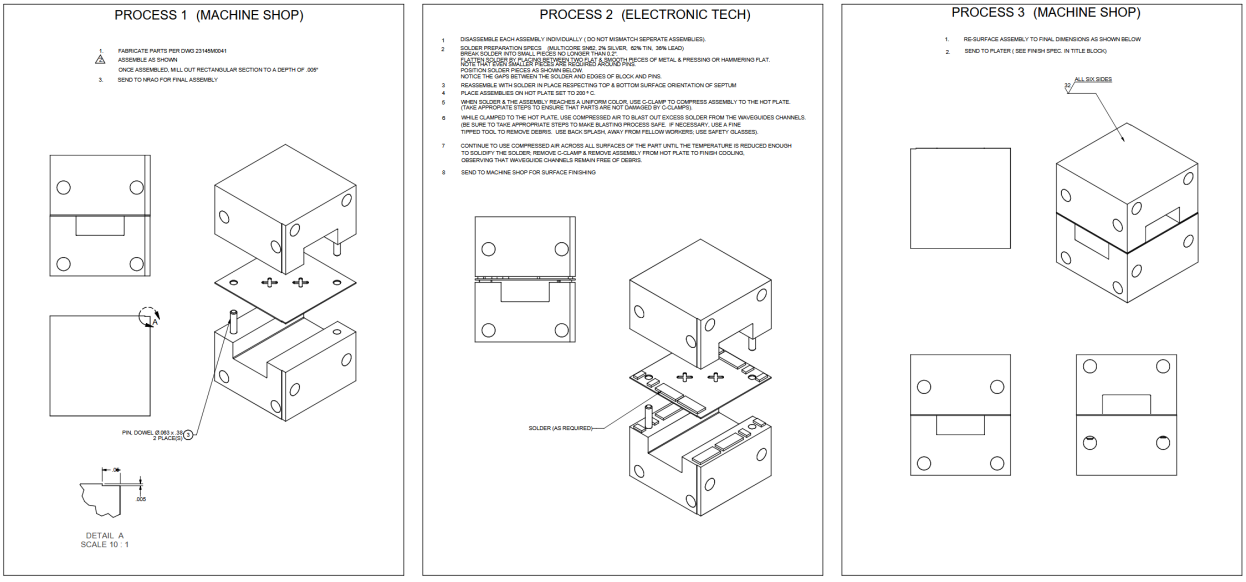

Figure 6. K-band cross-guide coupler assembly procedure

New Rev A Designs

Mechanical Design

Two new designs were conceived that use fasteners instead of solder to assemble the blocks and aperture plate. The two designs are shown in Figure 7.

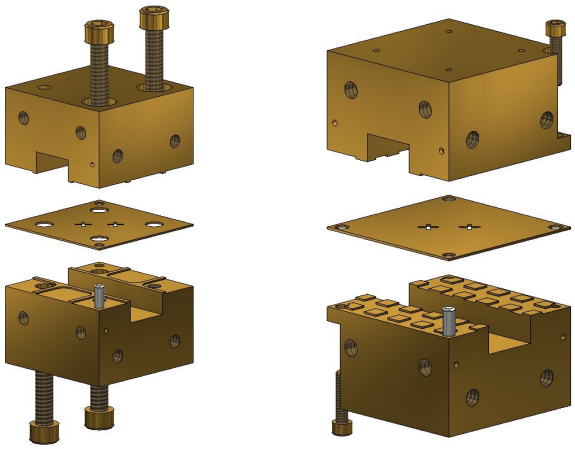

Figure 7. New Rev A coupler designs: "Clamped" (left) and "Waffled" (right)

The two new designs are as follows:

1) *"Clamped" (002.05.01.05.01-0010, Rev A).* Material is removed from each of the blocks in order to reduce the contact surface area, which enables improved flatness over the plane of contact and increased contact force per unit area. This is done in an effort to minimize gaps along the H-plane. Four 4-40 screws clamp the three parts together.

2) *"Waffled" (002.05.01.05.01-0011, Rev A).* A two-dimensional photonic crystal joint (PCJ) resembling a waffle-iron is utilized to prevent electrical currents from propagating into the joints, suppressing fields in the joints, and thus eliminating the effect of the joint [5]. Individual pillars are formed using direct machining in a pattern, creating a periodic 2-D array of reflecting elements with λ/4 periodicity at the center wavelength. The dimensions are based on [5] as shown in Figure 8, with waveguide width *a*. Optimum periodicity is 0.56*a* for square pillars, with side lengths of 0.28*a*. Rows are staggered with respect to each other by half a period. Only two rows are used in the cross-guide coupler design due to space constraints. The parts are held together using two 0-80 screws. While larger screws were desired, these are the only size to fit in the allotted space.

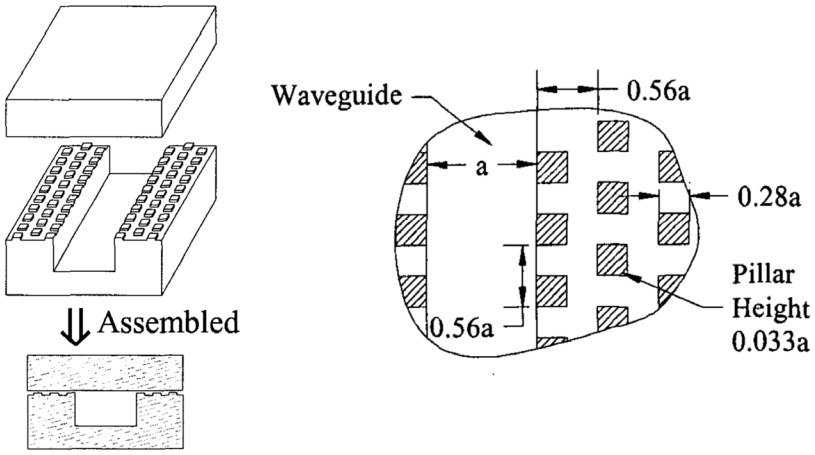

Figure 8. Photonic Crystal Joint metal pillars formed on one piece (left) and physical dimensions (right) [5]

Each part is machined from Brass. Brass screws are used for assembly in order to minimize effects of differential thermal contraction when cooled to cryogenic temperatures. Each of the 3 parts is plated in pure, soft Gold, which deforms when clamped, filling residual gaps across the mating surfaces.

Simulation

Each of the designs was initially modeled and simulated in Ansys HFSS with the following setup:

- Driven Modal Solution with 4 wave ports
- Adaptive Mesh Frequency = 40 GHz with Maximum Delta S = 0.001
- Discrete Sweep 26.5 to 40 GHz in 0.1 GHz steps (136 points)

The models are shown in Figure 9. All metal shapes are defined as Gold, with electrical conductivity 4.1×10^7 S/m. In reality, the screws are brass, the alignment pins are stainless steel, and the blocks are made of brass then gold plated. This is a simplifying assumption, but should have very little impact on the simulated results. Air is defined where metal does not exist. No surface roughness is defined. Wave ports are drawn at each of the waveguide ports on the device. Note that HFSS will introduce a perfect electrical boundary (PEC) around the structure as drawn.

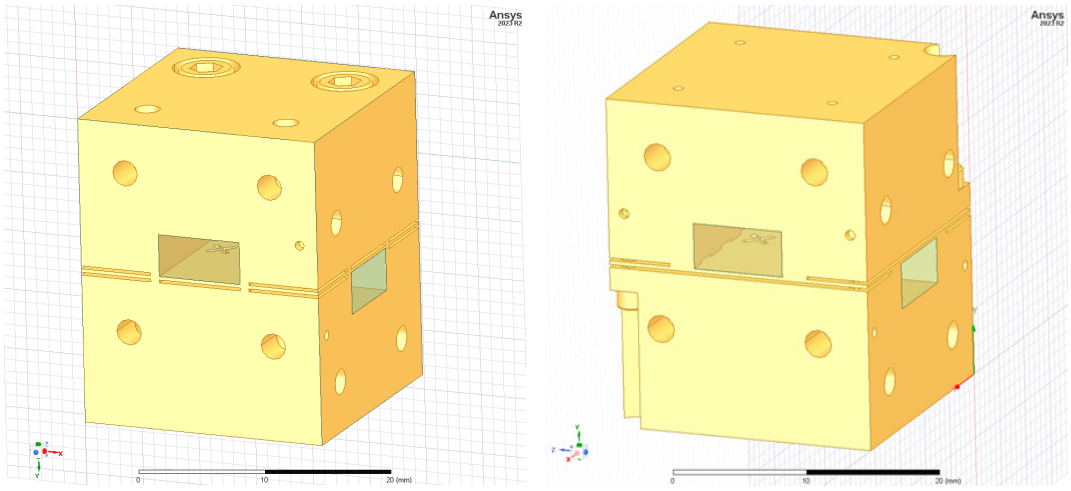

Figure 9. HFSS models for Rev A "Clamped" (left) and "Waffled" (right) cross-guide couplers

Convergence is achieved with 36148 tetrahedra elements in the clamped design and 42259 elements in the waffled design. While there are some small differences in the simulation results, they are very comparable. The results are shown in Figure 10.

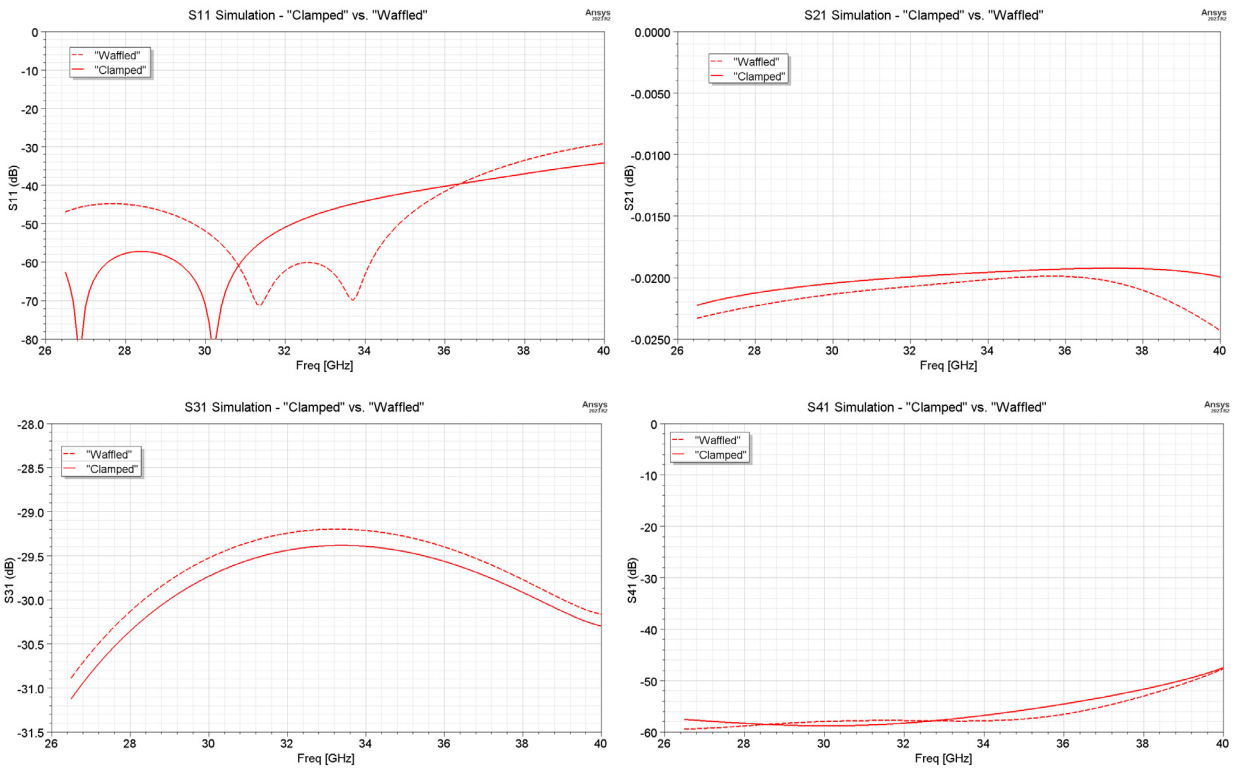

Figure 10. Initial s-parameter simulation of Rev A "Clamped" (solid) and "Waffled" (dashed) cross-guide couplers

Next, a gap along the H-plane between one of the blocks and the thin aperture plate was simulated in each of the designs. In this model, a radiation boundary is added around the component with an offset of 0.111 inches (~λ/4 at 26.5 GHz), and WR-28 waveguide PEC surfaces are added to extend to the radiation boundary faces. The "Clamped" model is shown in Figure 11. Gaps could manifest in many ways, but for the purposes of simplicity and simulation, a constant gap across the entire block is modeled.

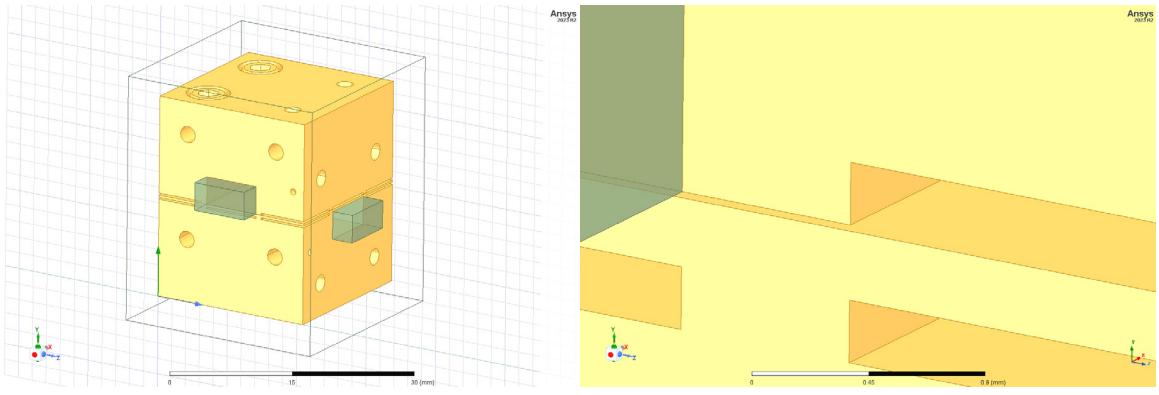

Figure 11. HFSS model for H-plane gap simulation of "Clamped" design (left) and close-up view showing gap (right)

The new model with a small parameterized gap requires many more mesh elements and takes longer to converge. Max delta S was relaxed to 0.005 to reduce simulation time, without a significant change in simulation results.

The gap is swept for both the “Clamped” and “Waffled” designs and the results are shown in Figure 12 and Figure 13, respectively, with the same scale. According to the simulation, the “Clamped” design remains better than 0.1 dB in S21 only up to a gap of 0.0001 inches, while the “Waffled” design still achieves this performance with roughly a gap of 0.001 inches. Thus, the “Waffled” design is much more tolerant to gaps in the H-plane, as expected.

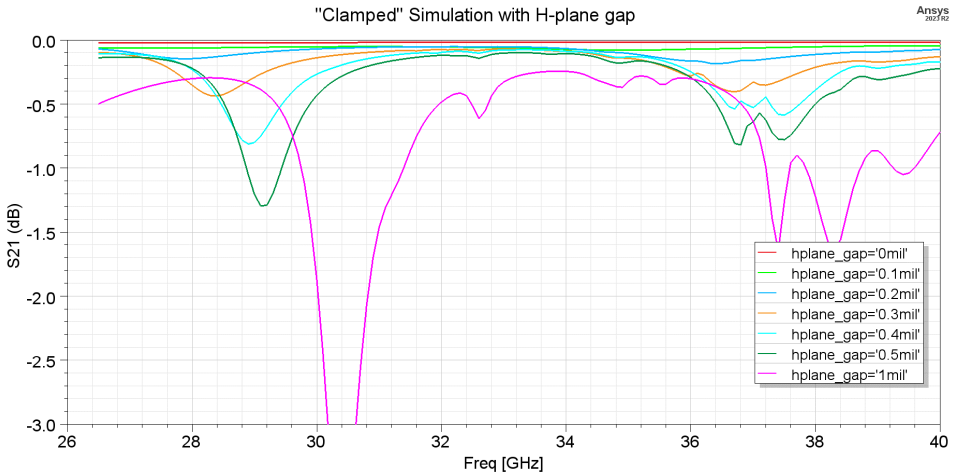

Figure 12. S21 (Thru) simulation of “Clamped” design for specified gaps along the H-plane split

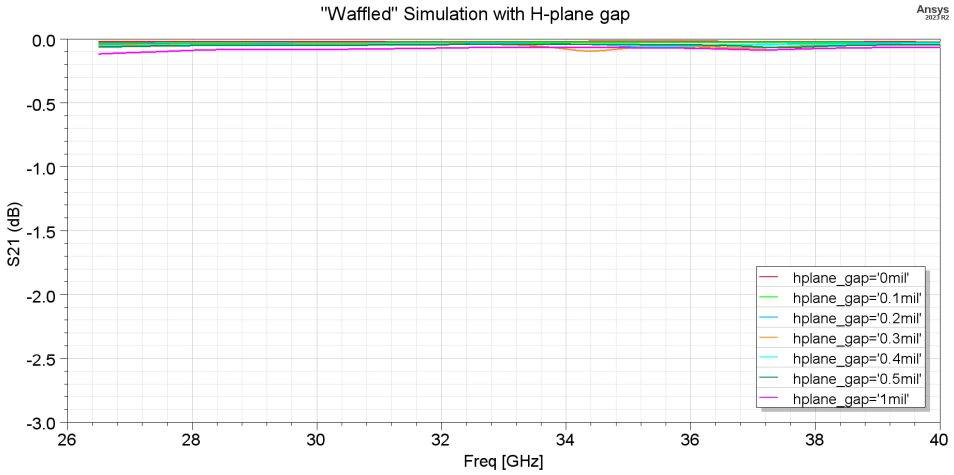

Figure 13. S21 (Thru) simulation of “Waffled” design for specified gaps along the H-plane split

Component Measurements and Experiments

The 3 parts for each variant were fabricated at the Central Development Laboratory (CDL) machine shop and gold plating lab in Charlottesville, VA. The parts for the “Clamped” and “Waffled” designs are shown in Figure 14.

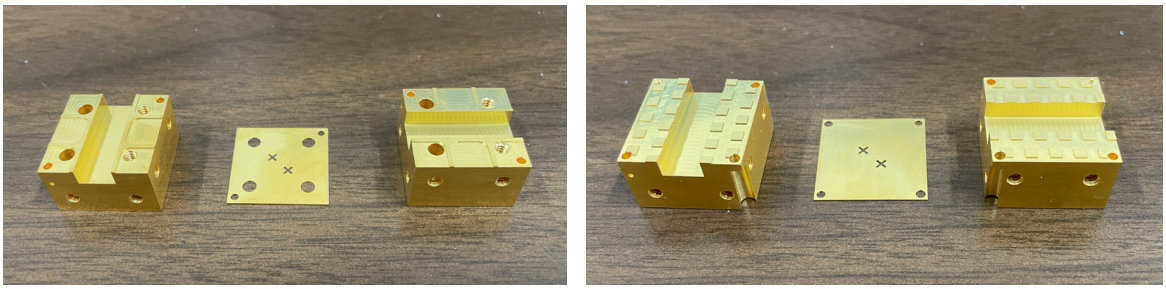

Figure 14. Parts for "Clamped" (left) and "Waffled" (right) assemblies

The torque to apply to each of the screws was analyzed, considering the contact area, yield strength of Gold, a target yield of 8%, a coefficient of friction of 0.14, and the tensile strength of the brass screws. In the "Clamped" design, torque per screw was calculated as 0.9175 in-lbf and for the 0-80 screws it was 0.168 in-lbf. A torque wrench was unavailable for these desired torques. Instead, the screw was turned by a calculated angle after it was seated in the tapped hole to achieve the desired torque.

One of each variant was built up for initial testing on the 2-port Rohde and Schwarz ZNA50 Vector Network Analyzer (VNA). TRL calibration to the device under test (DUT) input and output planes was completed using the Agilent R11644A WR-28 calibration kit. Aerowave 28-2000Au terminations were placed on ports not connected to the VNA. Images of the DUT in place for testing are shown in Figure 15.

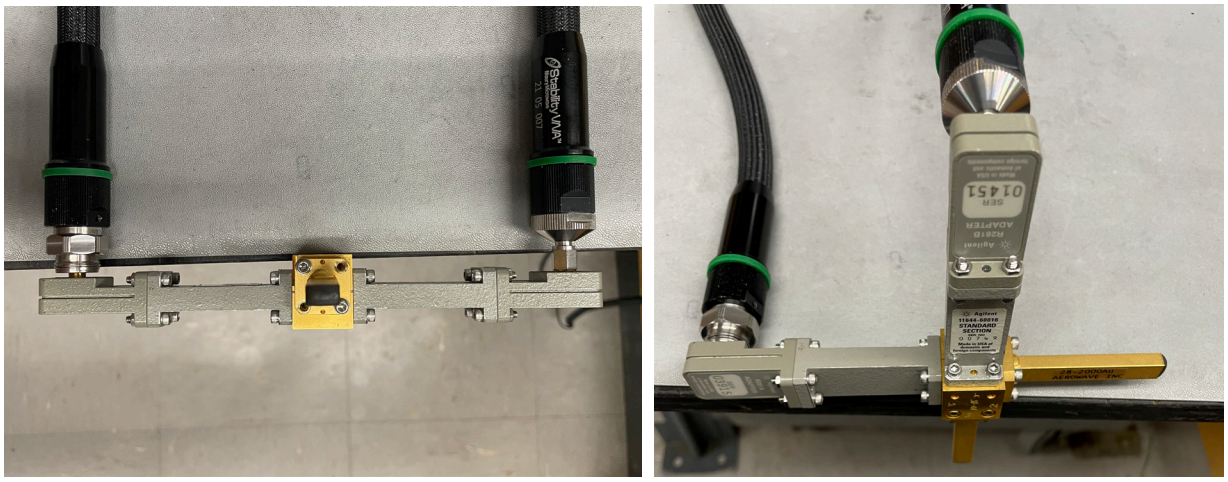

Figure 15. Directional coupler DUT measured on VNA: Thru path (left) and Coupled path (right)

The results for each device showed a resonance in the measured thru and coupled paths. The S21 for each of the devices for one measured Thru path is shown in Figure 16. Note that there is some variability in this measurement on each mating of the waveguide flange and on the 2 Thru paths for each device that can be measured.

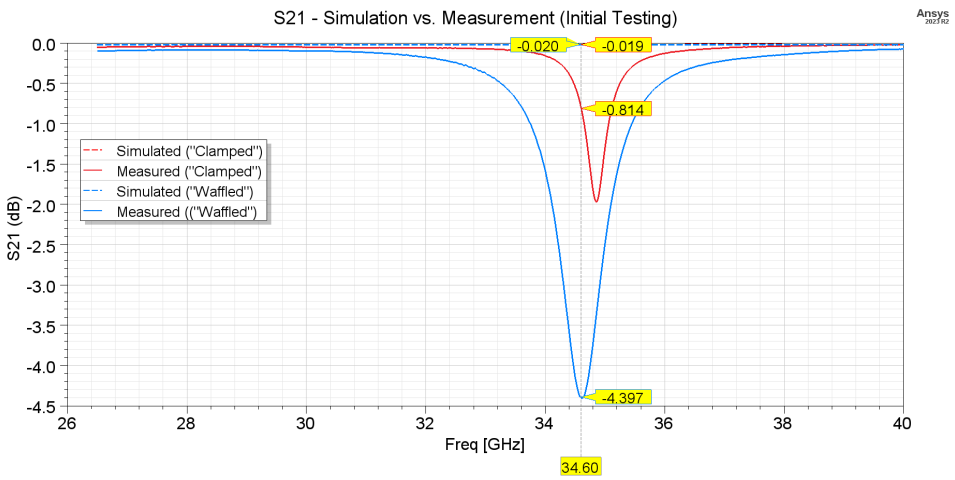

Figure 16. S21 (Thru) simulation vs. measurement, for initial assembled units

Flatness across the waveguide flanges was first identified as a possible cause of the resonance. During testing, it was noted that the three parts were very close, but not identical in size and that there appeared to be a lot of sensitivity and variability in the measurement when attaching and re-attaching the waveguide input to the DUT. Unlike the soldered design, we rely on the machining outer dimension of the parts to set the flatness, as the waveguide flange faces are not re-surfaced after assembly. This was done purposefully to simplify fabrication, but it remained a concern.

An attempt to loosely model this effect was implemented in HFSS. This was done by introducing a WR-28 waveguide section on input and output ports for each of the models and reducing the outer dimension of the coupling aperture plate from the nominal 0.820 inch by a very small amount. A waveguide flange is added on the input and output ports. The model is shown in Figure 17. The reduction in dimension was swept from 0 to 0.0015 inches in 0.0005 inch steps. This creates a very small "gap" where the waveguide meets the coupler device. This type of gap is different from those in the H-plane simulated previously.

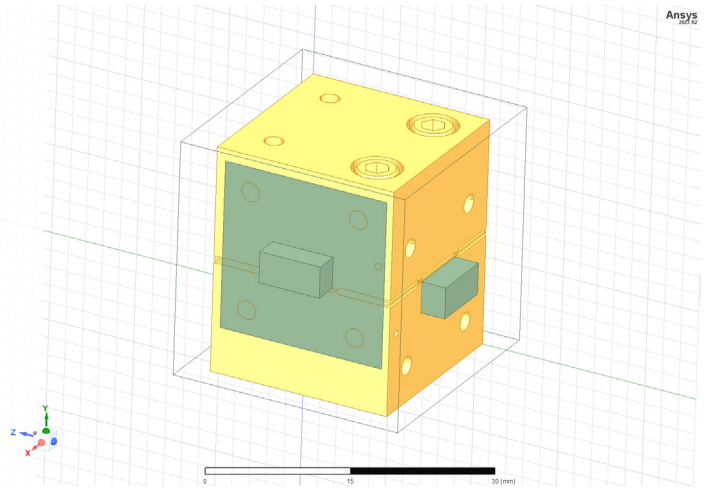

Figure 17. HFSS model for "Clamped" design with small gap introduced at the aperture plate

A comparison of the simulation to a measurement for S21 of the “Clamped” model is shown in Figure 18. Note that the same simulation solution mesh and sweep settings as used in the H-plane gap simulation are applied here.

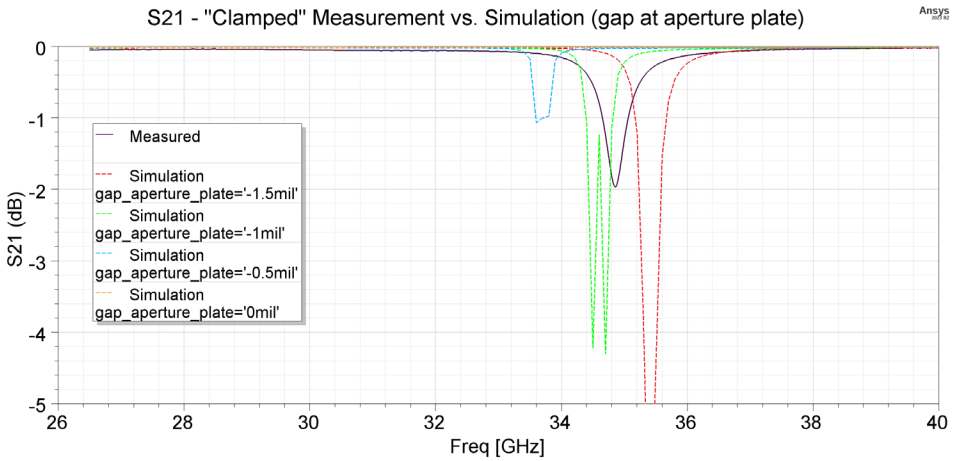

Figure 18. S21 (Thru) simulation (with gap at Aperture Plate) vs. measurement, “Clamped” design

While the measured behavior is not identical to the simulation, it does appear that there is some correlation. The simulation is just a rough approximation to the real physical build and the gaps that actually manifest. This simulation was repeated on the “Waffled” design and similar results were found. The simulation showed that the gap at this interface allowed for coupling into the “slot” below the waveguide. Another simulation was completed that shows that even with a gap, when this slot is covered with metal, the resonance in the response is eliminated. As a test, a modification was made to each of the physical designs to add Indium metal in an attempt to mostly seal this slot. This is shown for the “Clamped” design in Figure 19.

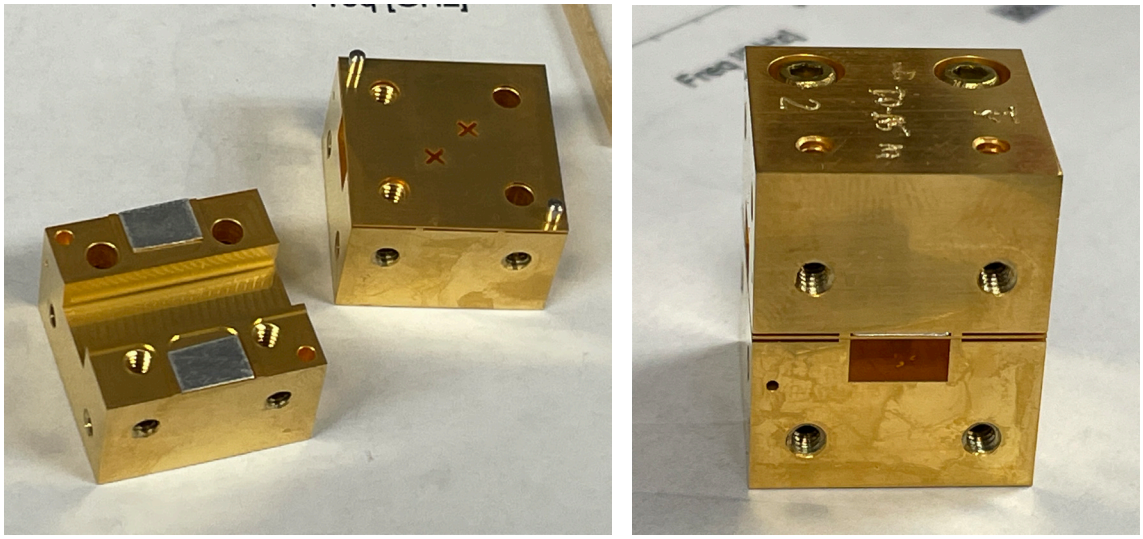

Figure 19. Filling slot with Indium for “Clamped” design

The unit was re-measured and the resonance was dramatically improved as shown in Figure 20. There still appears be a bit of degradation here at the high end of the band, which may be because the Indium fill of the slot is pretty good, but not perfect – there are still some gaps that energy can couple into.

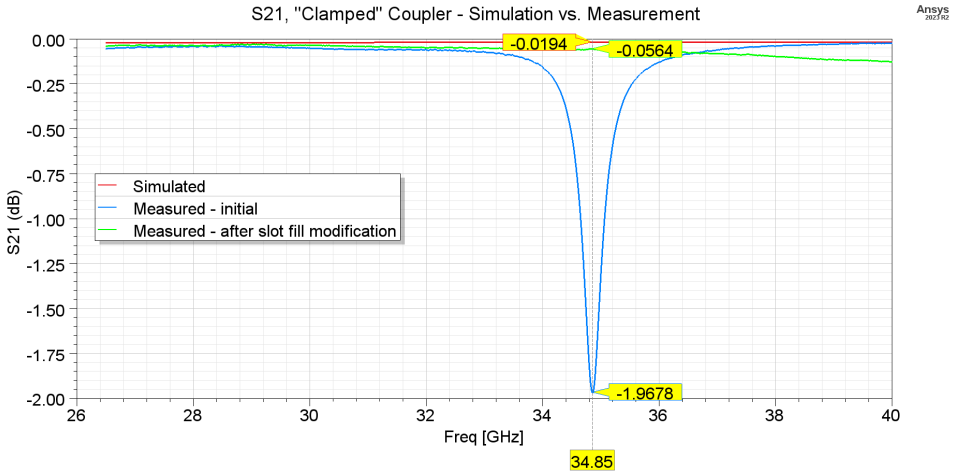

Figure 20. S21 (Thru) simulation vs. measurement of "Clamped" design (before and after modification)

Coupling S31 and Isolation S41 were also measured for this modified unit. Simulation vs. measurement is shown in Figure 21.

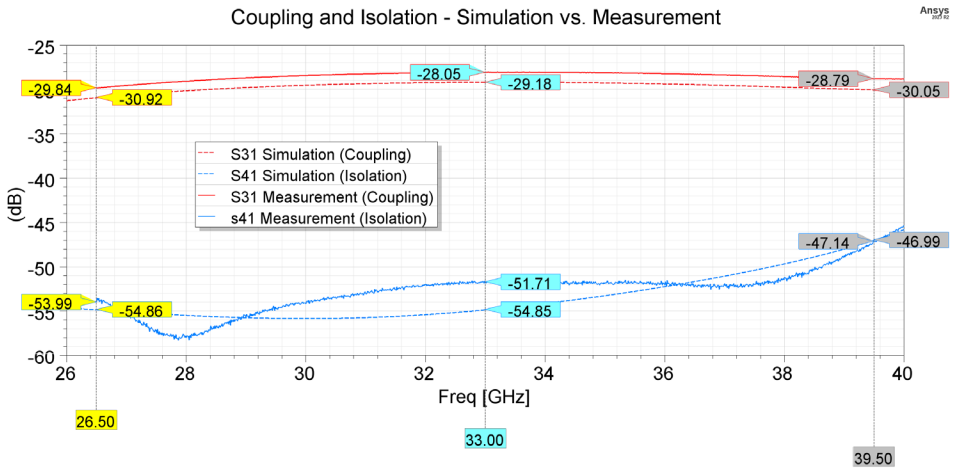

Figure 21. S31 (Coupled) and S41 (Isolated) simulation vs. measurement of "Clamped" modified design

Coupling was measured to be 1-1.5 dB higher than simulation. This could be a result of manufacturing variation due to tolerance, or some other small modeling error. Isolation was worse than simulation over the frequency band, but the max value matched simulation quite well. Note that this isolation was measured "directly" from port 1 to port 4 with the other ports terminated and thus return loss at the termination ports can increase the power measured at port 4. It is possible that this is one cause for the deviation between simulation and measurement.

Receiver Measurements

The modified "Clamped" unit was tested in an EVLA Ka-band receiver serial number 8 in order to see if the design would perform well in an actual cryogenically cooled receiver. Initially, the baseline receiver

performance was tested with the existing coupler, followed by a swap to the new component and re-testing. This was done on the Left-Hand Circularly Polarized (LCP) path. The receiver testing uses the "Y-factor" method to measure the receiver noise temperature T_{Rx}, which requires a measurement of noise power at 2 known load temperatures. Room temperature (~295K) and cold liquid nitrogen (~77K) loads are placed on the feed horn. The Y_{factor} and T_{Rx} are defined as:

$$Y_{factor} = \frac{Power_{hot}}{Power_{cold}}$$

$$T_{Rx} = \frac{T_{hot} - Y_{factor} * T_{cold}}{Y_{factor} - 1}$$

The test results are shown in Figure 22.

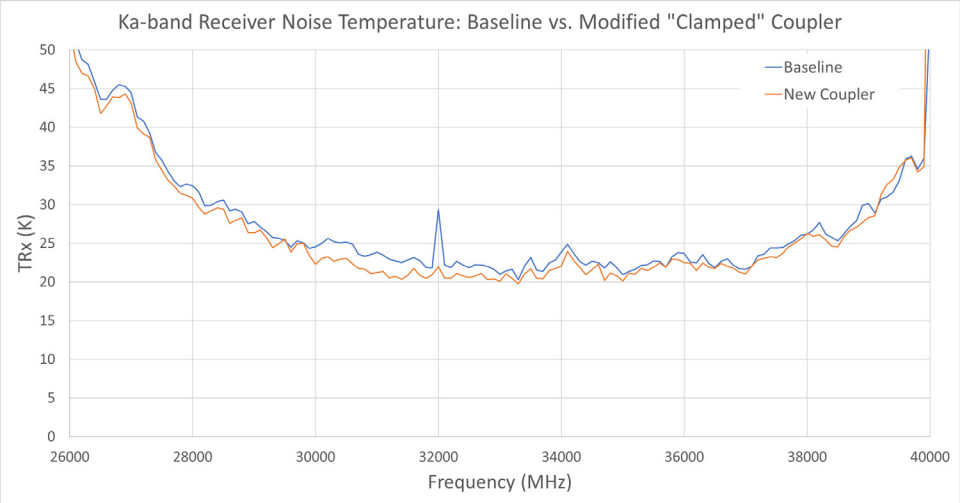

Figure 22. Ka-band receiver noise temperature measurement – baseline vs. new modified Rev A "Clamped" design

The measured results are close - while it appears that there are some small differences over frequency between the baseline and the new coupler, these may be due to uncertainty in the measurement. Some causes of uncertainty are:

- Hot and cold load is assumed invariant and fixed at 295K and 77K, respectively. The actual temperature of the hot load can vary based on the temperature in the room. The cold load can vary due to ambient temperature and humidity, dwell time of the liquid nitrogen before beginning test, and the possibility of frost forming on the load.
- The test frequency range is broken up into 2 separate tests requiring the cold and hot loads to be changed out 2 times each. The loads will have some variability from test to test.
- The ambient environment temperature can drift during testing, changing the response of the test rack equipment or receiver gain.
- Mechanical variability in testing, such as connecting and disconnecting cables and opening up the receiver enclosure can create inconsistencies in measurements.

- Cold stage temperature varies, due to factors such as uncontrolled helium pressure in the loop from test to test.

For example, a 1 K uncertainty in the cold load results in a 1.5 K uncertainty in receive noise temperature. A 0.1 dB drift in gain or power measurement results in an uncertainty of 1.2 K. A few Kelvin of uncertainty in the receive noise temperature can easily be arrived at due to some of these factors.

Rev B Design

A new revision was designed for the "Clamped" version only. The "Waffled" version is more complex to machine and assemble, but did not appear to provide a clear benefit over the "Clamped" version.

Revisions from Rev A

Issues and design changes for Rev B "Clamped" version are shown in Table 1.

Table 1. Issues in Rev A design and Rev B revisions

Issue	Description	Revision
1	The "slots" or "pockets" near the waveguide on both designs create an unacceptable in-band resonance.	Remove pocket-shaped cavities by adding a wall along the waveguide slots and a drilled hole for venting.
2	The alignment pins are slip-fit on all 3 pieces.	Change to anti-symmetric press and slip fit pins on blocks.
3	The alignment pins force incorrect orientation different from original design. The assembly is not a drop-in replacement.	Mirror the aperture locations on the plate.
4	Machined markings on the parts for port names/numbers, and version are desired for easy assembly and tracking.	Add port names "LNA", "OMT", "N.S.", "LOAD" and part revision marking.
5	The flatness across the waveguide flange face is a concern, since the new design is not surfaced flat after assembly.	Change tolerances to +/-.001 inch and add a surface flatness callout of 0.0005 inch across those faces.
6	Measured coupling is about 0.5dB higher than previous device. This is a minor difference and not a cause for concern. Current tolerances on the part allow for large variations in coupling.	Simplify and tighten aperture width and length dimensions specifications. All size and location tolerances are now +/-0.0005 inch.
7	Naming of the thin plates for the old designs are inconsistent and confusing.	Rename to "Coupling Aperture Plate"
8	Torqueing screws requires flipping over the part.	Change location of the screwed holes so there are 2 transverse on each side.
9	"Clamped" design allows for waveguide flange screws to rotate into and the deform the clamping screws.	Counterbore depth reduced. Able to avoid this issue on half of the flange screws.
10	Lock washers were absent in the design	Add "Split Lock Washers for Socket Head Screws." These will protrude above the top of the counterbore, but not interfere with next level assembly.

The old drawing tolerances allowed for a large variation in coupling and directivity performance, allowing for up to a variation of 11 dB nominal in coupling factor. New drawing tolerances (assumed uniform) for aperture width, length, and location were simulated over 100 statistical trials. The variation in coupling is now about 2.5 dB, which is small enough that the variation can be compensated for with the attenuator component in the noise calibration path. A histogram for coupling at 40 GHz is shown in Figure 23.

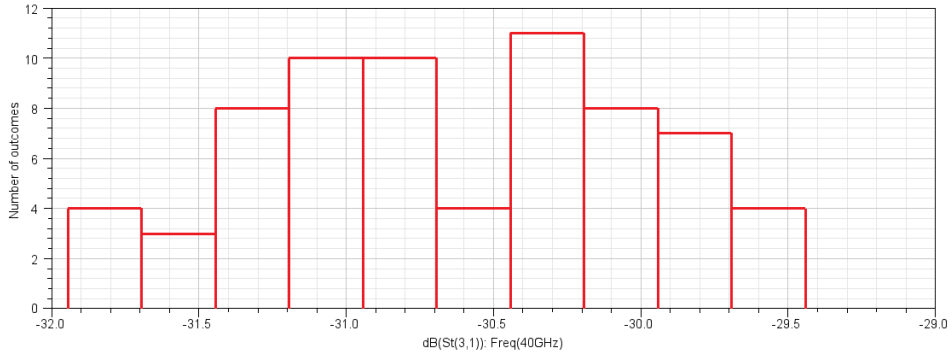

Figure 23. S31 (Coupled) simulation at 40GHz of 100 trials with new +/-0.001 inch tolerances

Directivity is typically greater than 20 dB but degrades at the high end of the band. Over 100 trials, the minimum is about 13 dB, as shown in Figure 24.

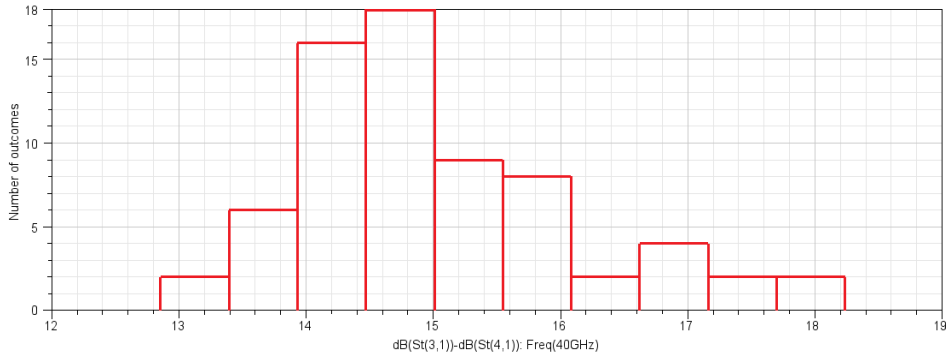

Figure 24. Directivity simulation at 40GHz of 100 trials with new +/-0.001 inch tolerances

Simulation

The revised “Clamped” Rev B exploded view is shown in Figure 25.

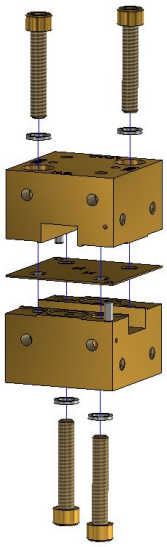

Figure 25. Rev B “Clamped” coupler design

The H-plane gap for Rev B was simulated, as was done in Rev A, with S21 transmission results shown in Figure 26. The results are similar to Rev A. This is expected – no design changes were made to improve performance with an H-plane gap. The testing on the initial Rev A units did not indicate that H-plane gaps were present.

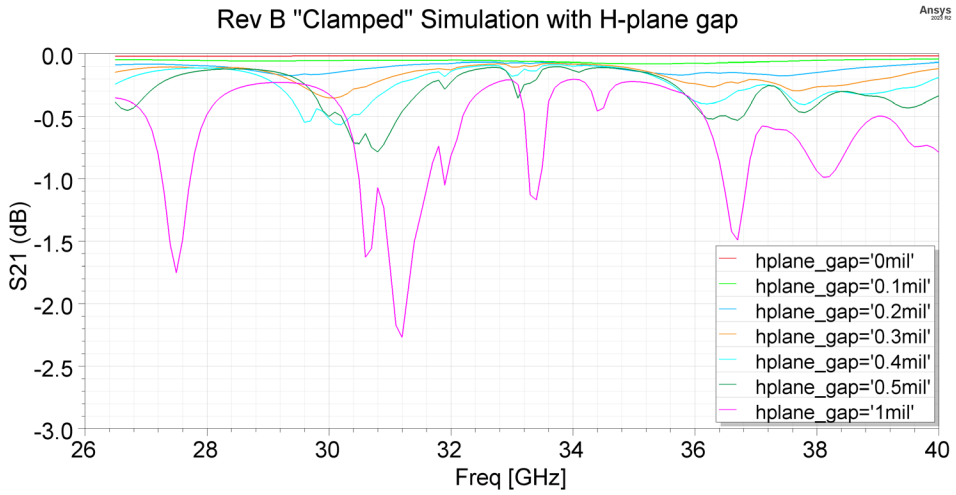

Figure 26. S21 (Thru) simulation of "Clamped" Rev B design for specified gaps along the H-plane split

Next, a small gap at the waveguide flange was introduced by decreasing the length and width of the aperture plate, as was done with the Rev A design. The simulation result is shown in Figure 27. With the new Rev B design, there is essentially no change in simulation with these small gaps. This indicates that the original issue was addressed with our design changes. Note that if the gap gets very large at this interface, performance in the simulation will start to degrade.

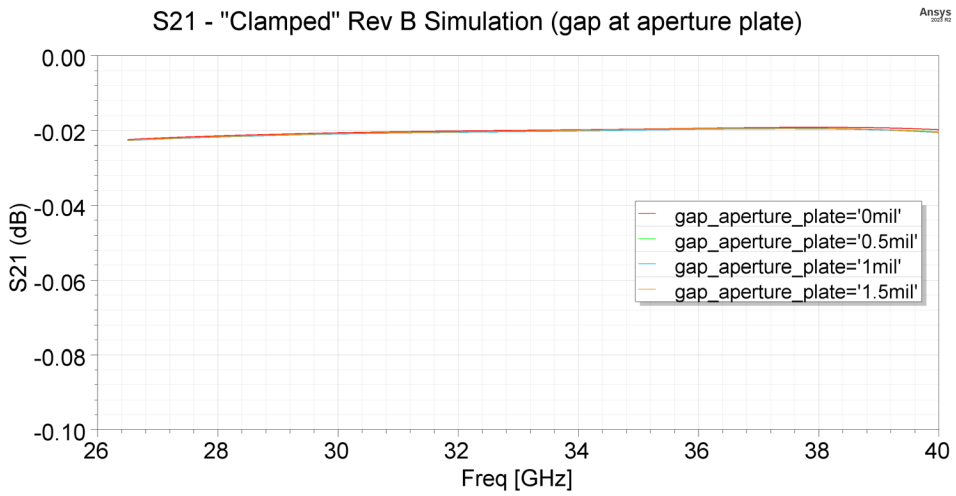

Figure 27. S21 (Thru) simulation (with gap at aperture plate) of Rev B "Clamped" design

Component Measurements

Four assemblies serialized SN001-004 were built using a torque screwdriver to set the torque on each brass screw to 2 in-lb. The torque was increased from the Rev A version due to the increase in contact surface area. A built assembly is shown in Figure 28.

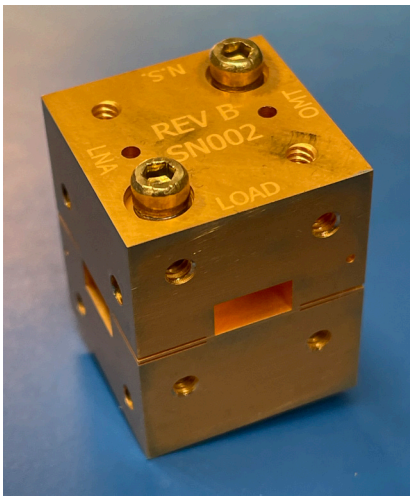

Figure 28. Rev B "Clamped" coupler assembly, SN002

The 4 assembled units were each measured on the Rohde & Schwarz ZNA50. Initial calibrated results across the 4 units showed that SN001 achieved the best performance. After further analysis, it was found that the initial calibration was not as good as desired. Re-calibration, followed by re-measurement of units SN002-SN004 was carried out. (SN001 was already installed in a receiver when the 2nd set of measurements commenced).

A comparison of simulation and measurement for return loss on the thru port (S11), transmission (S21), coupling (S31), and isolation (S41) are shown in Figure 29, Figure 30, Figure 31, and Figure 32 respectively. For additional information, these measurements and simulations show results over a wider bandwidth than earlier simulations.

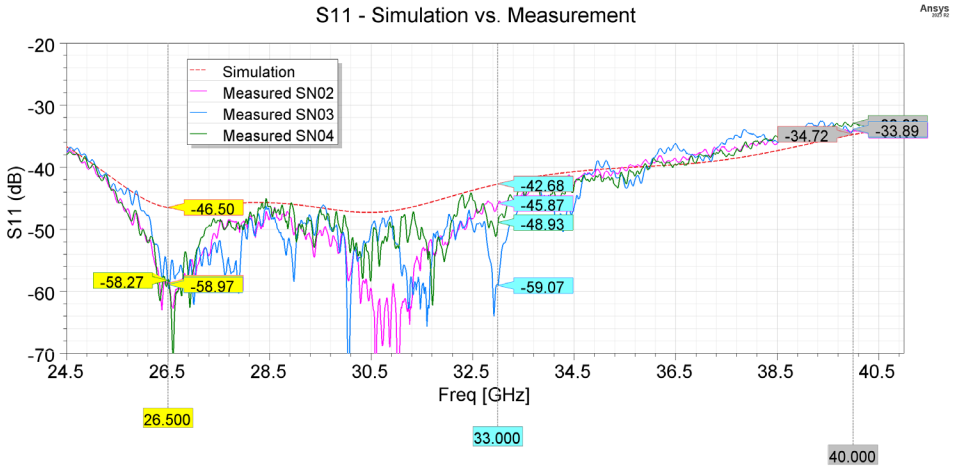

Figure 29. S11 (Return Loss, Thru Port) simulation vs. measurement of Rev B "Clamped" design

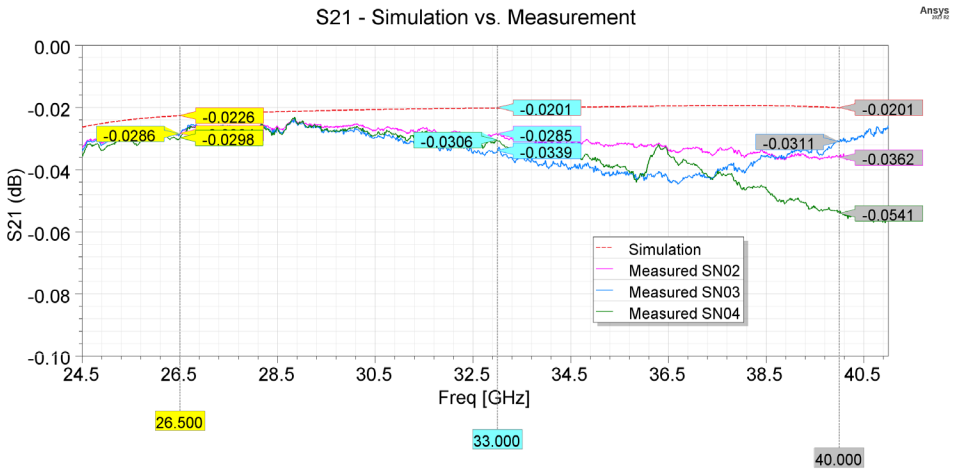

Figure 30. S21 (Thru) simulation vs. measurement of Rev B "Clamped" design

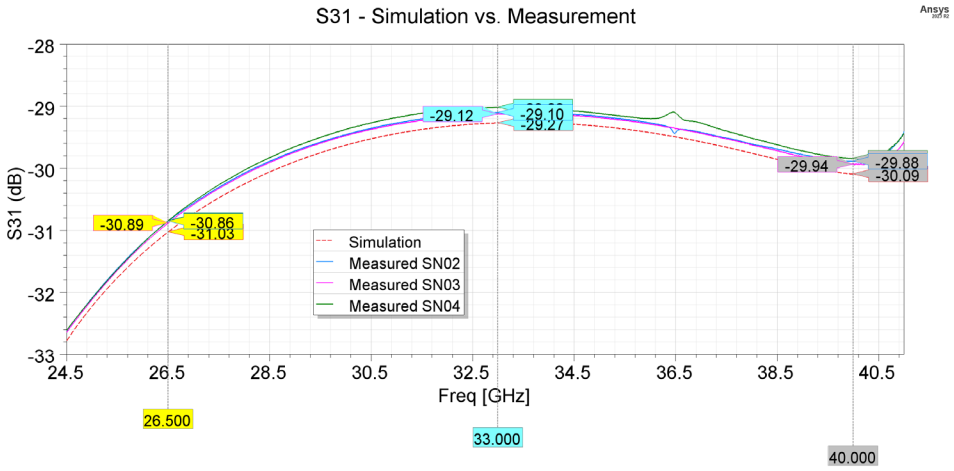

Figure 31. S31 (Coupled) simulation vs. measurement of Rev B "Clamped" design

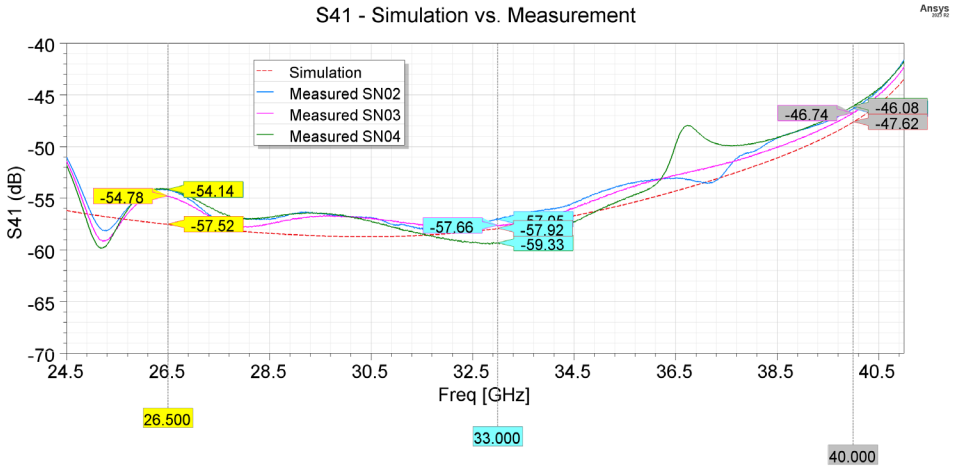

Figure 32. S41 (Isolated) simulation vs. measurement of Rev B "Clamped" design

The new components have quite good performance, similar to simulation. It was noted that there still appears to be some sensitivity to an in-band resonance and potentially a small increase in insertion loss in the higher frequencies in the band. This may be due to the same effect (aperture + cavity) that was observed in Rev A, however, the resonance, when it did appear, was very shallow.

Receiver Measurements

Baseline performance on Ka band receiver serial number 23 was taken. The receiver was then warmed up and opened to swap out the directional coupler on the LCP polarization with a Rev B SN001 unit and cooled again. The comparison in performance is shown in Figure 33.

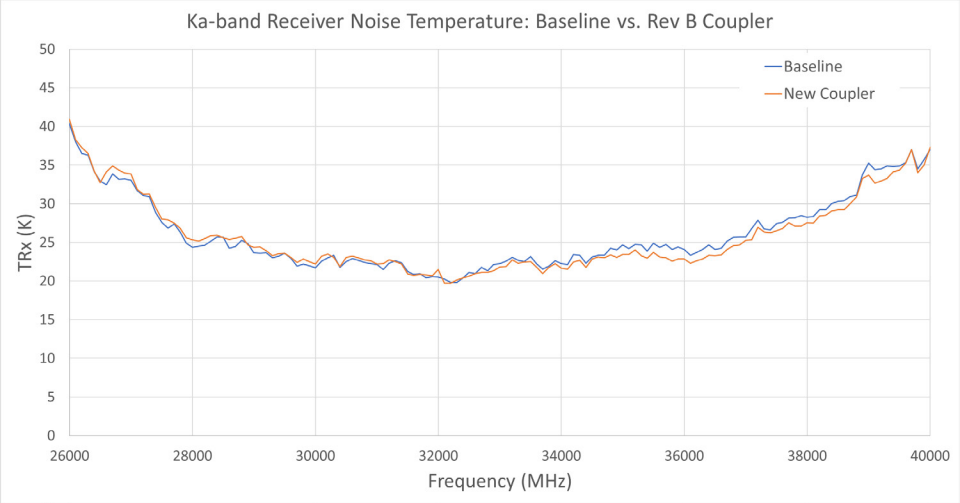

Figure 33. Ka-band receiver noise temperature measurement – baseline vs. new Rev B coupler

Antenna Measurements

Ka-band receiver serial number 23 calibration data file was updated on 4/9/24 as the receiver was tested in the screen room. The receiver was installed in antenna ea-26 in the Antenna Assembly Building and ea-26 was brought out to the Master Pad on 6/10/24. Re-commissioning of the antenna continued on the Master Pad until 7/5/24. The antenna was moved to BW8/W32 on 7/10/24.

To verify performance at the antenna and array level, stress test results were reviewed on 7/9/24-7/22/24. T_{sys} as reported on the stress test for antenna 26 LCP (IF C and D) was found to be "good," with values lower than the mean across the 28 antennas, ignoring any outliers as shown in Table 2.

Table 2. Stress Test results for Antenna 26 with new coupler installed

Date	**Weather**	**Source**	**T_{sys} (K) Antenna 26**	**T_{sys} (K) Mean (remove outliers)**
7/9	Partly Cloudy	1153+805	60.5	63.2
7/11	Clear	0217+738	57.5	60.2
7/15	Partly Cloudy	1153+805	56	62.1
7/16	Mostly Clear	0217+738	60.5	63.4
7/19	Partly Cloudy	1153+805	65	66.3
7/22	Mostly Cloudy	0217+738	62.5	64.4
7/25	Partly Cloudy	1800+784	61.5	64.9

Additionally, fringes and the RF sync detect ratio (SDR) were monitored during this time frame. Fringe amplitudes were in the expected range and looked "good." SDR (T_{cal}/T_{sys}) was ~3.1% during the 7/25 stress test.

Proposed Further Improvements to the Design

For future versions of the design, the following are proposed:

1) Reduce size of the "cavity" in the parts in order to increase the cavity resonance frequency to above the cut-off of rectangular waveguide. This should eliminate susceptibility to minor in-band resonances that can occur due to small gaps at the waveguide flange interface. The proposed change is shown in Figure 34.

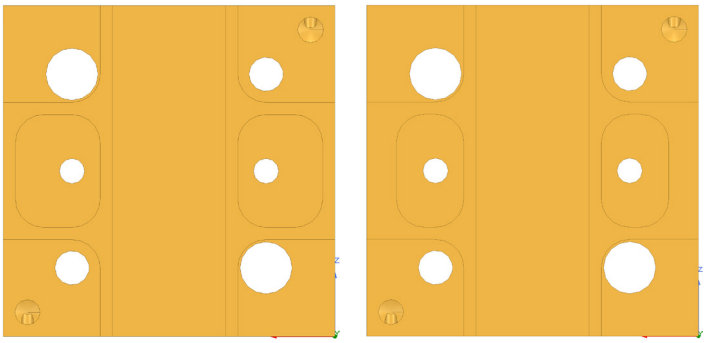

Figure 34. Coupler block cavity comparison - original (left) and reduced size (right)

2) Review dimensions and tolerance stack-up. There may be some inadvertent forces applied when assembled which can lead to a slightly bowed aperture plate.

Summary

A cross-guide coupler assembly was designed and built using fasteners to assemble the blocks and aperture coupling plate. A good correlation between simulation and measurement at the component level was achieved. Measured noise temperature results in a Ka-band receiver were as expected. The performance of this receiver in an antenna on the array was also verified. This design was conceived for Ka-band, but could be scaled for use in other frequency bands as well.

Conclusions from this work are as follows:

1) Close control of fabrication tolerances for a cross-guide coupler are important to achieve target coupling performance.
2) Careful attention needed to be paid to small gaps at the input and output waveguide interfaces, which caused cavity resonances to occur. In the initial design, only the gaps at the H-plane interfaces were identified as a concern and simulated.
3) Photonic crystal joint (PCJ) in the "waffled" design did appear to work as expected, but deemed unnecessary in this particular design. The "waffled" design is more complex to machine and needed to use very small 0-80 screws to fit in the allowable volume.
4) These designs were drop-in replacements on the EVLA receivers. For other applications, the volume constraints could possibly be relaxed, to allow more room for the screws used for assembly and mating flange attachment.

Acknowledgements

Thank you to:

- D. Urbain: Component design review, suggestions, and feedback.
- J. Ramzel: EVLA Ka-band receiver assembly and testing. Coupler assembly and testing.
- B. Simkin: Coupler modifications, testing, suggestions, and feedback.
- R. Long: VLA receiver and array interferometry data review.
- G. Morris and CDL machine shop: Fabrication of parts.

References

[1] R. Hayward and et al, "Chapter 5: Receivers," The VLA Expansion Project: Construction Project Book, National Radio Astronomy Observatory, 2007.

[2] A. Moreno, "A new directional coupler for waveguide," Sperry Gryoscope Eng. Rep., Sperry Gyroscope Co., 1946.

[3] J. Ball and T. Sulda, "Small aperture crossed waveguide broad-wall directional couplers," IEE Proc. Microw. Antennas Propag, vol. 147, no. 4, 2000.

[4] E. Barnett and J. Hunton, "A Precision Directional Coupler Using Multi-Hole Coupling," Hewlett Packard Journal, vol. 3, no. No 7-8, 1952.

[5] J. Hesler, "A photonic crystal joint (PCJ) for metal waveguides," IEEE MTT-S International Microwave Sympsoium Digest (Cat. No.01CH37157), vol. 2, pp. 783-786, 2001.